Research Paper

Global metabolomics analysis of serum from patients with Niemann−Pick disease type C

Anna Iwahori[1,†], Masamitsu Maekawa[1,2,3,†,*], Yoshitomi Kanemitsu[2,††], Yotaro Matsumoto[1,2,3], Yoshihisa Tomioka[1,2,3], Aya Narita[4], Torayuki Okuyama[5], Yoshikatsu Eto[6], Daisuke Saigusa[2,7], Nariyasu Mano[1,2,3]

[1] Faculty of Pharmaceutical Sciences, Tohoku University, 1−1 Seiryo-machi, Aoba-ku, Sendai, Miyagi 980−8574, Japan
[2] Department of Pharmaceutical Sciences, Tohoku University Hospital, 1−1 Seiryo-machi, Aoba-ku, Sendai, Miyagi 980−8574, Japan
[3] Graduate School of Pharmaceutical Sciences, Tohoku University, 1−1 Seiryo-machi, Aoba-ku, Sendai, Miyagi 980−8574, Japan
[4] Division of Child Neurology, Tottori University Hospital, 86 Nishi-machi, Yonago, Tottori 683−8503, Japan
[5] Department of Clinical Laboratory Medicine, National Center for Child Health and Development, 2−10−1 Okura, Setagaya-ku, Tokyo 157−8535, Japan
[6] Advanced Clinical Research Center, Institute for Neurological Disorders, 255 Furusawa-Miyako, Asou-ku, Kawasaki, Kanagawa 215−0026, Japan
[7] Department of Integrative Genomics, Tohoku Medical Megabank Organization, Tohoku University, 2−1 Seiryo-machi, Aoba-ku, Sendai, Miyagi 980−8575, Japan

Abstract Niemann−Pick disease type C (NPC) is an autosomal recessive disorder with a wide clinical spectrum. NPC is caused by a lack of cholesterol transport proteins. In recent years, various lipid-derived biomarkers for NPC have been identified, suggesting extensive abnormal metabolism of various lipids. Global metabolomics is a technique that enables qualitative and semi-quantitative analysis based on accurate mass spectrometry combined with liquid chromatography. It is also useful for identifying biomarkers. In this study, a global metabolomics approach was applied to serum from patients with NPC to clarify lipid metabolism abnormalities. Serum samples were analyzed by liquid chromatographic separation with gradient elution and high-resolution mass spectrometry. After post-processing, all datasets were subjected to multivariate analysis. Principal component analysis showed overlapping of sample groups between healthy subjects and NPC patients. Orthogonal partial least square-discriminant analysis detected characteristic peaks corresponding to metabolites such as *N*-palmitoyl-*O*-phosphocholine-serine and sphingosylphosphorylcholine, which have previously been reported as biomarkers of NPC. Novel changes in levels of metabolites such as lysophosphatidylinositol were also observed in NPC, and peaks indicating the existence of a novel metabolic pathway, involving metabolites such as *N*-acylserine, were also detected. These results indicate that global metabolomics is useful for comprehensive analysis of metabolic changes in NPC pathology.

[†] These authors contributed equally to this work.
[††] Current address: Clinical and Translational Research Center, Niigata University Medical and Dental Hospital, 1−754 Asahi-machi dori, Chuo-ku, Niigata, Niigata 951−8122, Japan

[*] **Corresponding author**
Masamitsu Maekawa
Department of Pharmaceutical Sciences, Tohoku University Hospital, 1−1 Seiryo-machi, Aoba-ku, Sendai, Miyagi 980−8574, Japan
Tel: +81−22−717−7541, Fax: +81−22−717−7545
E-mail: m-maekawa@tohoku.ac.jp
Received: January 16, 2020. Accepted: April 14, 2020.
Epub May 27, 2020.
DOI: 10.24508/mms.2020.06.006

Key words: Niemann−Pick disease type C, Global metabolomics, mass spectrometry, LC/MS/MS, lipids

Abbreviations: LC/MS, liquid chromatography/mass spectrometry; NPC, Niemann−Pick disease type C; PPCS, *N*-palmitoyl-*O*-phosphocholine-serine; SPC, sphingosylphosphorylcholine; SQC, study quality control

Introduction

Niemann−Pick type C (NPC) is an autosomal recessive disorder with an incidence of approximately 1/100,000−120,000[1,2]. A wide clinical spectrum is one of the hallmarks of this disease[3], with visceral, central nervous system, and psychiatric symptoms observed in clinical practice[1−3]. In addition, the scarcity of specialists for this disease presents a problem. Accordingly, the diagnosis of this disease is difficult. Conventional laboratory tests for NPC use filipin staining[4,5] and DNA sequencing[6]. Therefore, in recent years, many biomarkers for NPC have been chosen because they facilitate quick and simple analysis. Oxysterols[7], cholenic acid conjugates[8−10], lysophospholipids such as sphingosylphosphorylcholine (SPC)[11], and *N*-palmitoyl-*O*-phosphocholine-serine (PPCS)[12,13] have been reported as biomarkers for NPC so far. In general, disease biomarkers in the serum/plasma are generated by abnormal intracellular metabolism[14,15]. In the case of NPC, the causative genes are *NPC1*[16] and *NPC2*[17]. A functional lack of these cholesterol transport proteins causes cellular accumulation of cholesterol[1,18]. Oxysterols and cholenoic acid conjugates are thought to be produced from accumulated cholesterol by oxidative stress and metabolism[19,20]. Although sphingomyelin has been reported to bind cholesterol[21], its metabolic relationship with cholesterol is unclear. The structure of PPCS was determined recently[12,13], but its biosynthetic pathway has not yet been elucidated. These reports suggest that many metabolic

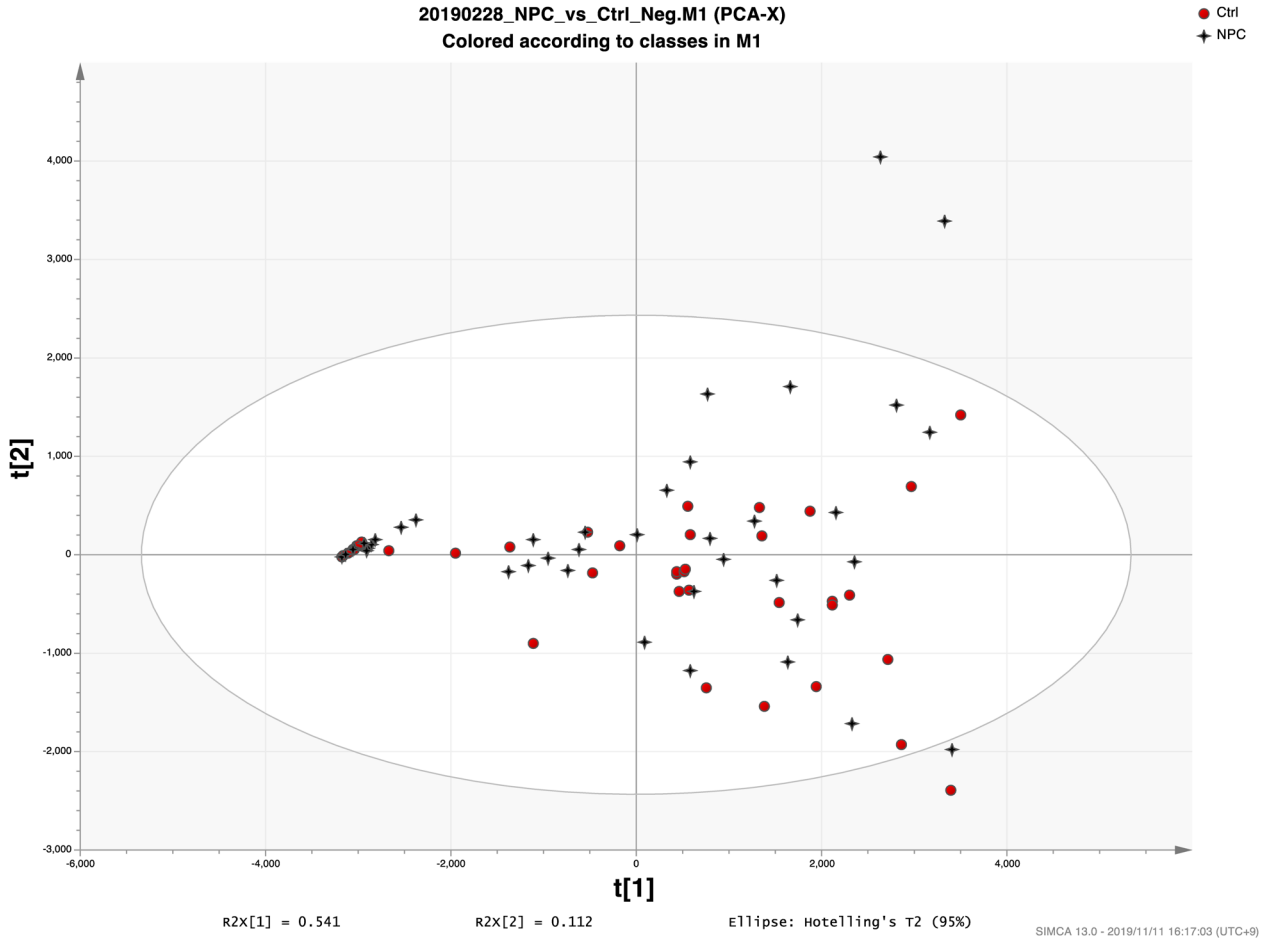

Fig. 1. Principal component analysis in negative ion mode.
Circle, control; cross, NPC.

abnormalities, not only those involving cholesterol, occur in NPC pathology. To clarify this matter, we analyzed serum samples, which are considered to be representative of intracellular metabolism. Global metabolomics[22] is a comprehensive analytical method for molecular identification and semi-quantitative analysis based on liquid chromatography (LC)/high-resolution mass spectrometry (MS), which is effective for analyzing metabolic abnormalities and searching biomarkers in various diseases[23,24]. In this study, we applied a global metabolomics method to analyze the serum of NPC patients and aimed to elucidate any comprehensive metabolic alterations.

Materials and Methods

Chemicals

Ethanol was purchased from Maruki Co. Ltd. (Sendai, Japan). Acetonitrile was purchased from Kanto Kagaku (Tokyo, Japan). Ammonium acetate was purchased from FUJIFILM Wako pure chemicals (Osaka, Japan). Ethylenediaminetetraacetic acid was purchased from Dojindo (Kumamoto, Japan). Ultrapure water was obtained from PURELAB Ultra Genetic (Organo, Tokyo).

Serum samples

Serum samples were obtained from patients with NPC (*N*=45) and healthy subjects (*N*=37) who provided informed consent. All experiments were performed in accordance with the Declaration of Helsinki principles and followed a protocol approved by the Ethics Committee of the Graduate School of Medicine in Tohoku University (approval number: 2013-1-293).

Sample preparation

Twenty microliters of a mixture of ethanol and water (3 : 1, v/v), 20 μL of an internal standard (IS) mixture (containing 1 μM PPCS-$^2H_3$ and lysosphingomyelin (d17:1)), and 50 μL acetonitrile were added to 10 μL of serum and mixed adequately. After centrifugation at 14,000×*g* at 4°C

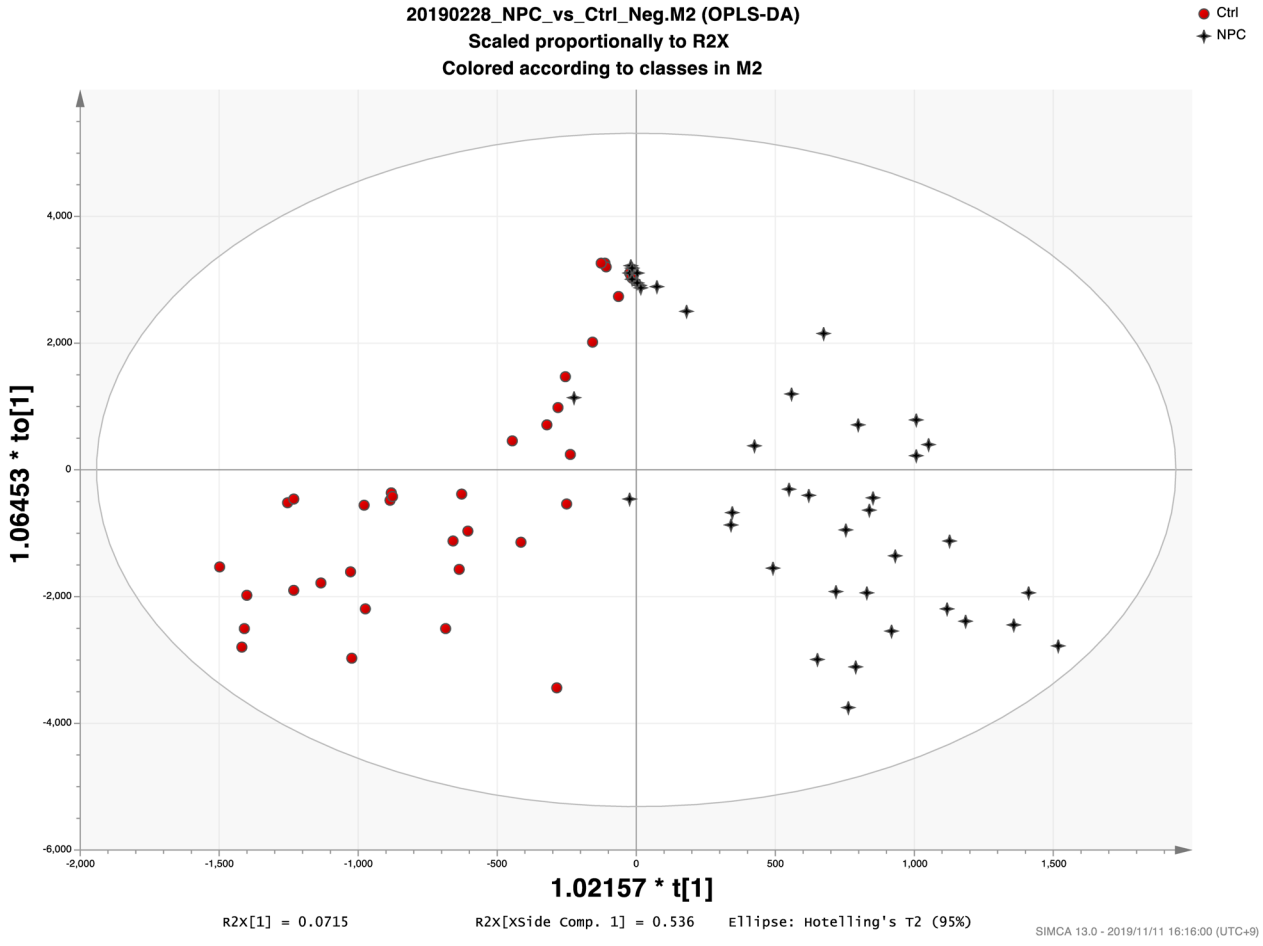

Fig. 2. Orthogonal partial least square-discriminant analysis in negative ion mode.
Circle, control; cross, NPC.

for 10 min, 3 μL of supernatant was injected into the LC/MS apparatus for analysis.

Sample preparation for quality control study

Serum (10 μL) was mixed and used as a study quality control (SQC). The SQC was combined with a mixture of formic acid and water (0.1 : 100, v/v) to produce two-fold (×2 SQC), four-fold (×4 SQC), eight-fold (×8 SQC), and 16-fold (×16 SQC) dilutions, respectively.

Analytical order in batch analysis

For the initial batch analysis, the SQC was analyzed 10 times. Eight of the prepared serum samples were analyzed. The analytical order of serum samples was randomized, regardless of whether the samples were from NPC patients or healthy controls. After every eight sample analyses, the SQC was analyzed. At the end of the batch analysis, diluted SQC samples were sequentially analyzed from ×16 SQC to SQC.

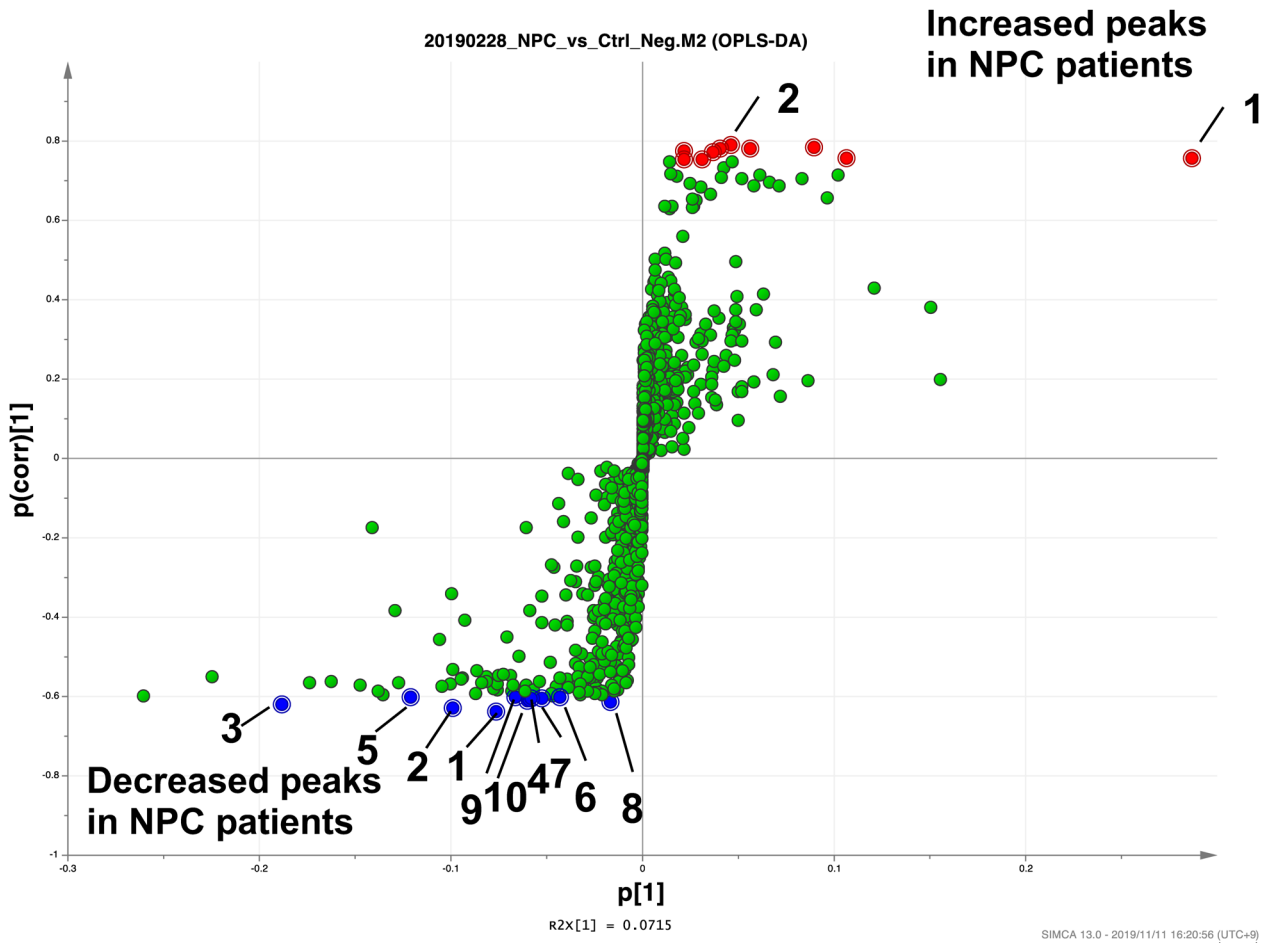

Fig. 3. S-plots in negative ion mode.
Red colored plots show the peaks increasing in NPC patients with p(corr)>0.75.
The peaks corresponding to No. 1 and 2 in Table 1 were marked.
Blue colored plots show the peaks decreasing in NPC patients with p(corr)<−0.60.
The peaks corresponding to No. 1−10 in Table 2 were marked.

Table 1. The peak list with p(corr)>0.75 on negative ion mode

No.	Retention time (min)	*m/z*	Formula	MS difference (ppm)	Candidate
1	16.52	507.3208	$C_{24}H_{49}N_2O_7P$	0.6702	*N*-Palmitoyl-*O*-phosphocholine-serine
2	16.53	565.2793	$C_{26}H_{49}O_{12}P$	1.6697	Lysophosphatidylinositol (17 : 1)

LC/MS analysis

LC/MS analysis was performed as described in a previous report with minor revisions[22]. The Orbitrap Fusion (Thermo Fisher Scientific, Waltham, MA, USA) and Vanquish systems were used for high-resolution tandem MS and ultra-high-performance LC. Positive and negative spray voltages were set to 3,500 V and −2,000 V, respectively. Sheath gas (arb), auxiliary gas (arb), sweep gas (arb), ion transfer tube temperature (°C), vaporizer temperature (°C), *m/z* range, resolution, and higher collision-induced dissociation energy (%) were set to 50, 10, 0, 275, 350, 200−1,500, 120,000, and 50%, respectively. An InertSustain Bio C18 column (2 μm, 150 mm×2.1 mm inner diameter, GL sciences, Tokyo) was used as the analytical column. Mobile phases A and B comprised 5 mM ammonium acetate in methanol/acetonitrile/water (1 : 1 : 3, v/v/v), and 5 mM ammonium acetate and 10 nM ethylenediaminetetraacetic acid in acetone/isopropanol (1 : 1, v/v), respectively. The program timings were set as follows: B (%) 0 to 100 over 40 min. The flow rate and column oven temperature were set to 0.3 mL/min and 40°C, respectively.

Data processing

Xcalibur software (Thermo Fisher Scientific) was used to perform LC/MS analysis and data collection. The collected data were loaded into Progenesis QI (Nonlinear Dynamics, Newcastle, UK). A dataset was provided for peak picking, alignment, and normalization of retention time and *m/z*. Protonated molecules, sodium adduct, potassium adduct, and ammonium adduct ions were selected on positive ion mode. Deprotonated molecules and acetic acid adduct ions were selected in the negative ion mode. All adduct ions attributed to the same molecules were deconvoluted and identified based on the human metabolome database and lipidmaps. Peaks for which the coefficient of variance of the peak intensity was greater than 30% were excluded from the data processing, as were peaks whose intensity did not change with the dilution factor.

Statistical analysis

The peak intensities were normalized by in-house quantbolome software using the SQC and IS peak intensities[22]. Multivariate analysis was performed for fitting, using principal component analysis (PCA) and orthogonal partial least square-discriminant analysis (OPLS-DA) with SIMCA version 13 (Umetrics, Umea, Sweden). *p*-values were calculated using the Wilcoxon rank sum test, and analysis of variance values were calculated using Progenesis QI.

Results and Discussion

PCA analysis of the negative ion mode

First, PCA analysis was performed after collection of LC/MS measurement data. Before the analyses, it was confirmed that there were no differences between the age and gender of healthy subjects and patients with NPC (data not shown). PCA analysis is useful for characterizing all samples. If the plots forms the cluster, it means that the samples included in the same cluster have similar characteristics. As shown in Fig. 1, many overlaps were observed between the healthy control group (circle) and the NPC patient group (cross), suggesting that there were many common serum metabolites among the healthy controls and patients with NPC.

Table 2. The peak list with p(corr)＜−0.60 on negative ion mode

No.	Retention time (min)	*m/z*	Formula	MS difference (ppm)	Candidates
1	4.75	369.1742	$C_{19}H_{30}O_5S$	0.0927	Androsterone sulfate
2	6.52	369.1741	$C_{19}H_{30}O_5S$	0.0927	Androsterone sulfate
3	7.47	369.1741	$C_{19}H_{30}O_5S$	0.0927	Androsterone sulfate
4	9.08	369.1741	$C_{19}H_{30}O_5S$	0.0927	Androsterone sulfate
5	19.04	465.3588	$C_{28}H_{50}O_5$	0.5699	6α-Hydroxycastasterone
6	19.14	485.3851	$C_{31}H_{54}NO_4$	−4.6694	Arachidonyl carnitine
7	20.26	489.3578	$C_{30}H_{52}O_6$	−1.54	6β-Acetoxy-24-methylcholestan-3β,5α,22R,24-tetrol
8	20.63	467.3146	$C_{30}H_{46}O_5$	−4.2467	(3β,15α,22S,24E)-3,15,22-Trihydroxylanosta-7,9(11),24-trien-26-oic acid
9	21.25	491.3747	$C_{30}H_{52}O_5$	1.1204	25-Acetoxy-ergosta-3β,5α,6β-triol
10	23.49	615.4614	$C_{38}H_{64}O_6$	−2.6018	Triglyceride (35 : 4)

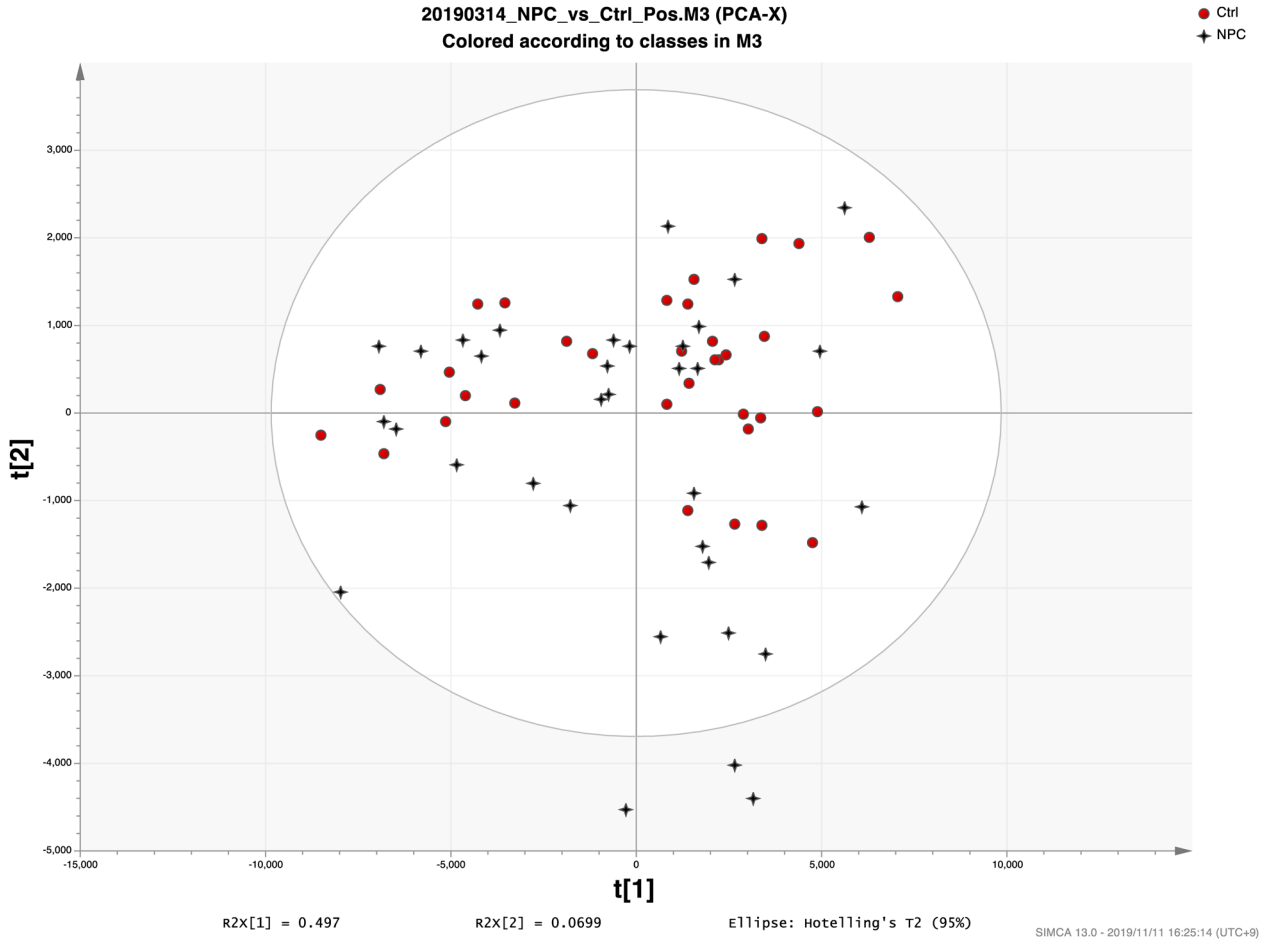

Fig. 4. Principal component analysis in positive ion mode.
Circle, control; cross, NPC.

OPLS-DA analysis of the negative ion mode

By contrast, when OPLS-DA analysis was performed, the two groups could be distinguished clearly (Fig. 2). In addition, an s-plot[25] was used to identify peaks that differed between the two groups (Fig. 3). The peaks located in the upper right of the plot indicate the metabolites that were increased in NPC patients, whereas the peaks located in the lower left correspond to metabolites whose levels were higher in healthy subjects. The value on the vertical axis (p(corr)) indicates the reliability of the peak, similar to a *t*-test result. The peaks with smaller p(corr) values tended to provide significant difference. The value (*p*) on the horizontal axis represents the intensity of a peak. Peaks with larger *p* values appeared on the left and right of the plot. In this study, we hypothesized that the metabolites that provided significant alteration regardless of changes in intensity could be useful for analyzing pathological changes in NPC. The peaks with p(corr) values greater than 0.75 were identified using the database and are listed in Table 1 (red plot located at upper right region in Fig. 3). Briefly, these peaks increased in NPC patients. The Peaks for which no suitable candidates were found were not included in Tables. Peak 1 represents a novel lipid that was recently identified as PPCS[12,13] and had the largest p(corr) value. This peak was identified as lysosphingomyelin-509 by Giese et al. in 2015[26]. The biosynthetic pathway of this metabolite has not yet been elucidated. *N*-acylphosphatidylserine[27,28] and *N*-acylserine[28] were speculated to be precursors, but their metabolites did not increase in the negative ion mode (Fig. 2 and Table 1). Peak 2 had an accurate mass corresponding to that of lysophosphatidylinositol (17 : 1). Phosphatidylinositols are speculated to be biomarkers of various cancers[28]. However, this metabolite contained an odd number of fatty acid chains; thus, the reliability of the peak identification was uncertain. The metabolites whose p(corr) values were lower than -0.6 are listed in Table 2. These peaks decreased in NPC patients, and they were shown as blue spots located in the lower left of Fig. 3. Peaks 1−4 had retention times of

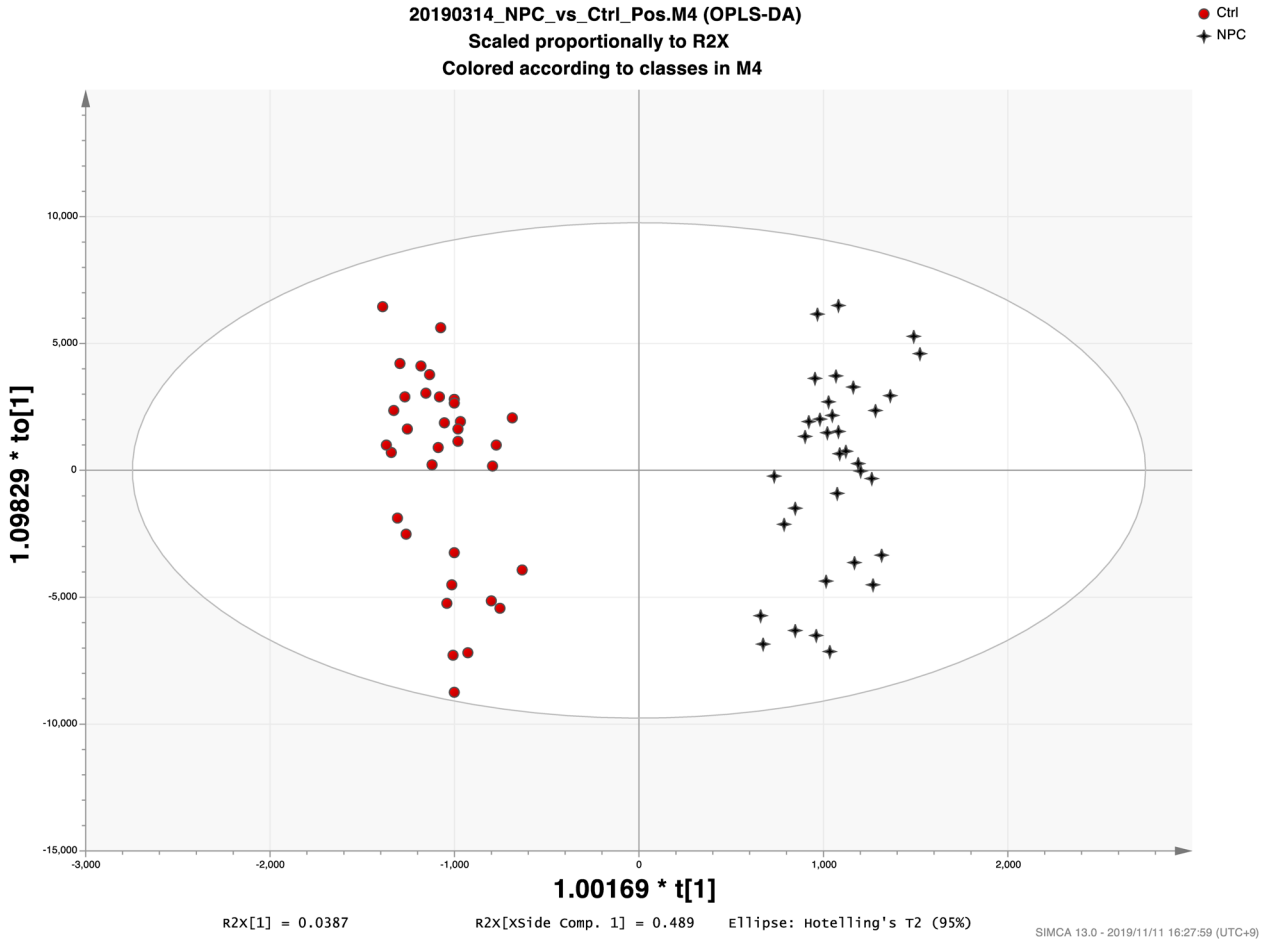

Fig. 5. Orthogonal partial least square-discriminant analysis in positive ion mode.
Circle, control; cross, NPC.

4.75−9.08 min and masses corresponding to androsterone sulfate and sulfate-conjugated steroid hormones. The metabolites of peaks 1−4 had equal mass and so were speculated to be structural isomers. Steroidal compounds are present in NPC patients; oxysterols and cholenoic acid conjugates have been reported[7−10,20]. It is possible that metabolism of steroid hormone sulfates might be affected in NPC patients. Peaks 5 and 7−9 were speculated to be sterol metabolites; however, their compound names were like sterol derivatives. As mentioned above, abnormalities in oxysterols and cholenoic acids have been reported in NPC. Peak 6 had a mass value corresponding to a metabolite classified as an acylcarnitine. Acylcarnitines are affected by mitochondrial functions. Peak 10 was speculated to be triglyceride (35 : 4), but its fatty acid chain length was relatively short (carbon number 35). Accordingly, it may be a diglyceride. No alterations in acylcarnitines and triglycerides have been reported in patients with NPC.

PCA analysis of the positive ion mode

In the positive ion mode, as was the case in the negative ion mode, a relatively large number of samples were plotted close to each other (Fig. 4).

OPLS-DA analysis of positive ion mode

Compared to the results for the negative ion mode, the two groups could be separated more distinctly in the positive ion mode (Fig. 5). The results of the s-plot are shown in Fig. 6. The peaks with p(corr)>0.60 and their identities are listed in Table 3. These peaks increased in NPC patients and are indicated by red plots which located at upper right in Fig. 6. Peak 1 was speculated to be lysophosphatidic acid (30 : 7). The metabolite of peak 2 was also a flavonoid compound; it was not evident that this was an NPC-specific metabolite. SPC (peak 3) is a sphingolipid metabolite that has been reported to be increased in NPC patients[11,12]. However, arachidonyl carnitine, corresponding to peak 4 (Table 2), was increased in NPC patients, cervonyl carni-

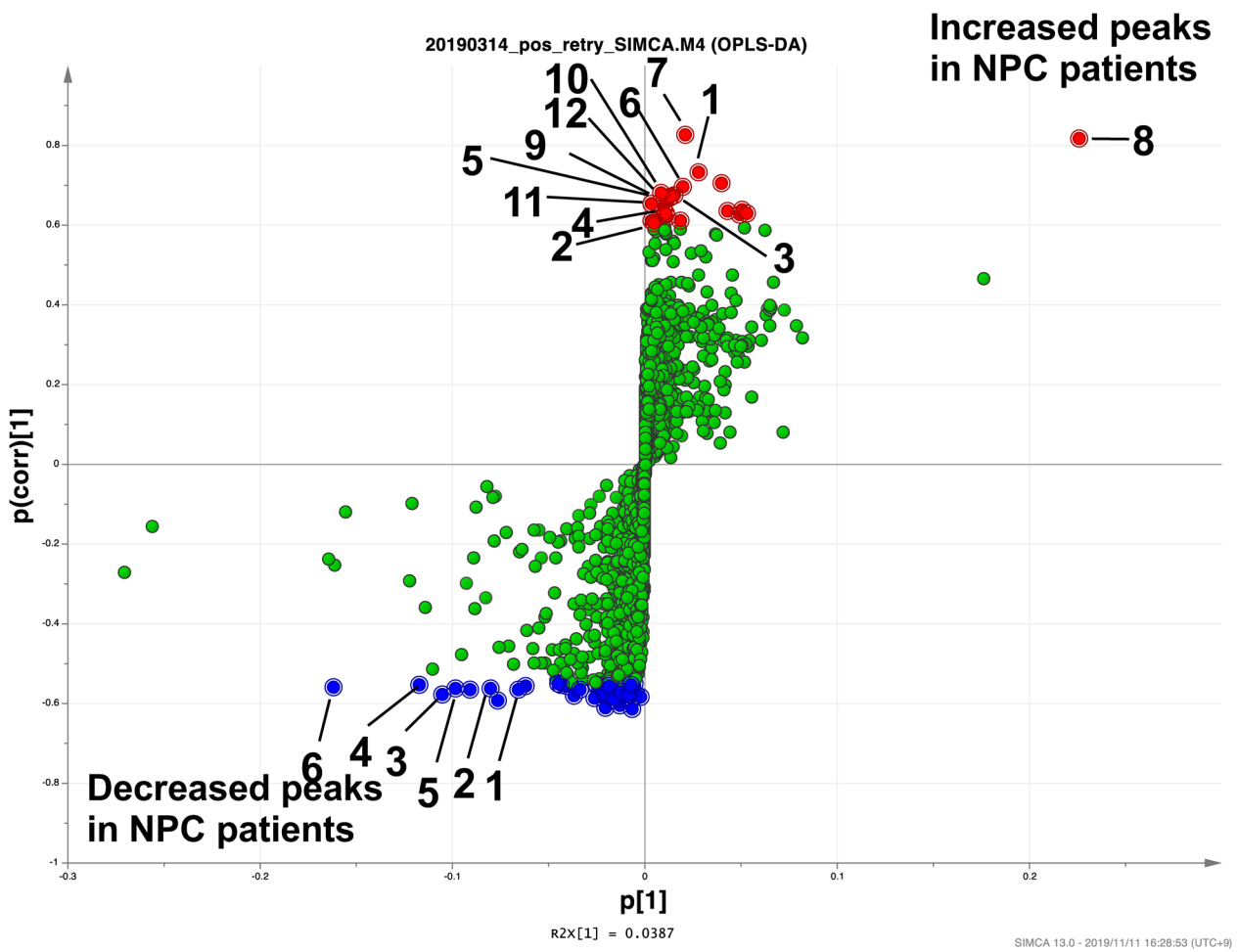

Fig. 6. S-plots in positive ion mode.
Red colored plots show the peaks increasing in NPC patients with p(corr)＞0.60.
The peaks corresponding to No. 1−11 in Table 3 were marked.
Blue colored plots show the peaks decreasing in NPC patients with p(corr)＜−0.55.
The peaks corresponding to No. 1−6 in Table 4 were marked.

Table 3. The peak list with p(corr)＞0.60 on positive ion mode

No.	Retention time (min)	*m/z*	Formula	MS difference (ppm)	Candidates
1	8.14	593.3558	$C_{33}H_{53}O_7P$	−7.4436	Lysophosphatidic acid (30:7)
2	10.49	495.126	$C_{26}H_{24}O_{11}$	−5.0927	3,4,5-trihydroxy-6-(2-{5-hydroxy-8,8-dimethyl-2-oxo-2H,8H-pyrano [2,3-f]chromen-4-yl}phenoxy)oxane-2-carboxylic acid
3	12.47	426.3686	$C_{23}H_{49}N_2O_5P$	−6.7193	Sphingosylphosphorylcholine
4	12.74	489.3684	$C_{29}H_{45}NO_4$	−0.4976	Cervonyl carnitine
5	12.77	431.3155	$C_{27}H_{44}O_5$	−0.2491	(6*R*)-6,19-Epidioxy-1α,25-dihydroxy-6,19-dihydrovitamin D3
6	14.37	597.3343	$C_{28}H_{55}O_{12}P$	−9.0018	Lysophosphatidylinositol (19:0)
7	16.30	509.3351	$C_{24}H_{49}N_2O_7P$	0.1571	*N*-Palmitoyl-*O*-phosphocholine-serine
8	16.37	553.2987	$C_{29}H_{44}O_{10}$	−3.6121	Desglucocheirotoxol
9	16.96	510.3193	$C_{24}H_{48}NO_8P$	0.4581	Lysophosphatidylserine (P-18:0)
10	19.59	559.3485	$C_{28}H_{48}NO_7P$	−4.0641	Lysophosphatidylcholine (20:5)
11	19.60	537.3663	$C_{26}H_{50}NO_7P$	0.0121	Lysophosphatidylcholine (18:2)
12	17.30	326.2687	$C_{19}H_{37}NO_4$	−0.6527	*N*-Palmitoyl serine

Table 4. The peak list with p(corr)<−0.55 on positive ion mode

No.	Retention time (min)	*m/z*	Formula	MS difference (ppm)	Candidates
1	21.96	586.5043	$C_{34}H_{64}O_6$	0.3688	Triglyceride (31 : 0)
2	23.86	640.5514	$C_{38}H_{70}O_{6*}$	0.4859	Triglyceride (35 : 1)
3	24.17	612.5199	$C_{36}H_{66}O_{6*}$	0.2139	Triglyceride (33 : 1)
4	24.72	614.5357	$C_{36}H_{68}O_6$	0.3835	Triglyceride (33 : 0)
5	24.96	642.5671	$C_{38}H_{72}O_6$	0.5641	Triglyceride (35 : 0)
6	32.35	742.5753	$C_{42}H_{82}NO_8P$	0.9857	Phosphatidylcholine (34 : 1)

tine, which is classified as an acylcarnitine, decreased (Table 3). Fatty acid groups might also affect to the difference. Peak 5 was speculated to be a vitamin D metabolite. No changes in vitamin D levels in NPC pathology have been reported. Phosphatidylinositol (peak 6) was also observed in the negative ion mode (peak 2 in Table 1). Peak 7 was also detected in the positive ion mode and identified as PPCS. Peak 8 corresponded to desglucocheirotoxol, with unknown origin. Ether-linked phosphatidylserine and *N*-palmitoylserine, which may be related to PPCS, were detected (peaks 9 and 12), in contrast to the negative ion mode. Peaks 10 and 11 were identified as lysophosphatidylcholine (20 : 5 and 18 : 2, respectively). In a previous report, levels of lysophosphatidylcholine with saturated fatty acids were decreased in NPC[13]; however, the alteration of unsaturated fatty acids has been not reported previously.

There were 6 metabolites which decreased in NPC patients (Table 4 and Fig. 6, blue plots located in lower left region). Five of the decreased peaks (Table 4) were classified as triglycerides (peaks 1−5). However, they all had an odd number of carbon chains; thus, further investigation is needed. Lysophosphatidylcholine increased (peaks 12 and 13, Table 3), and phosphatidylcholine decreased. In this study, lipid metabolites were detected mainly owing to the use of reverse-phase LC/MS. Changes in cholesterol, cholenic acid, sphingolipids, and *N*-acyl fatty acid metabolites have been reported in NPC; however, changes in other lipids, such as phosphatidylcholine, sterols, and vitamin D, were also detected in this study. As many lipid molecules exhibit biological activity, changes in these lipids may lead to further systemic physiological changes in NPC. It will be necessary to further analyze the relationships among lipid abnormalities, NPC pathology, and symptoms.

Conclusion

In this study, we used global metabolomics to analyze serum samples of NPC patients, in order to elucidate the molecular mechanism of abnormal lipid metabolism in NPC caused by mutations in cholesterol transport proteins. Many peaks were detected using an accurate MS system. Criteria for peak reduction based on SQC and DQC and multivariate analyses were used to focus on the significant peaks. As a result, many novel changes in lipid molecules containing phosphatidylinositols and *N*-acylserine were observed. Although the metabolic pathway of PPCS has not yet been elucidated, changes in *N*-acylserine and phosphatidylserine were observed. These metabolites are speculated to be precursors of PPCS[13]. These results were achieved by the excellent molecular identification and semi-quantitative analysis capabilities provided by a global metabolomics strategy. In the future, we intend to elucidate the detailed molecular mechanisms of the central metabolic pathways, as well as focus on biosynthesis using various cell lines.

Acknowledgments

We are grateful to all donors who provided serum and plasma samples, and to the doctors who collected serum samples. This work was supported in part by JSPS KAKENHI 18K15699, Japan AMED (JP19km0105001 and JP19km0105002) and by the Project for Promoting Public Utilization of Advanced Research Infrastructure (MEXT).

Conflicts of Interest

The authors declare no conflicts of interest.

References

1) Vanier MT: Niemann-Pick disease type C. *Orphanet J Rare Dis* 5: 16, 2010.
2) Geberhiwot T, Moro A, Dardis A, Ramaswami U, Sirrs S, et al: Consensus clinical management guidelines for Niemann-Pick disease type C. *Orphanet J Rare Dis* 13: 50, 2018.

3) Patterson MC, Hendriksz CJ, Walterfang M, Vanier MT, Wijburg F, et al: Recommendations for the diagnosis and management of Niemann-Pick disease type C: An update. *Mol Genet Metab* 106: 330−344, 2012.
4) Pentchev PG, Boothe AD, Kruth HS, Weintroub H, Stivers J, et al: A genetic storage disorder in BALB/C mice with a metabolic block in esterification of exogenous cholesterol. *J Biol Chem* 250: 5784−5791, 1984.
5) Vanier MT, Latour P: Laboratory diagnosis of Niemann−Pick disease type C: The filipin staining test. *Method Cell Biol* 126: 357−375, 2015.
6) Mckay K, Gissen BP: Genetic and laboratory diagnostic approach in Niemann Pick disease type C. *J Neurol* 261: S569−S575, 2014.
7) Porter FD, Scherrer DE, Lanier MH, Langmade J, Molugu V, et al: Cholesterol oxidation products are sensitive and specific blood-based biomarkers for Niemann-Pick C1 disease. *Sci Transl Med* 2: 56ra81, 2010.
8) Maekawa M, Jinnoh I, Narita A, Iida T, Saigusa D, et al: Investigation of diagnostic performance of five urinary cholesterol metabolites for Niemann−Pick disease type C. *J Lipid Res* 60: 2074−2081, 2019.
9) Maekawa M, Narita A, Jinnoh I, Iida T, Marquardt T, et al: Diagnostic performance evaluation of sulfate-conjugated cholesterol metabolites as urinary biomarkers of Niemann−Pick disease type C. *Steroids* 494: 58−63, 2019.
10) Maekawa M, Misawa Y, Sotoura A, Yamaguchi H, Togawa M, et al: LC/ESI-MS/MS analysis of urinary 3β-sulfooxy-7β-*N*-acetylglucosaminyl-5-cholen-24-oic acid and its amides: New biomarkers for the detection of Niemann−Pick type C disease. *Steroids* 78: 967−972, 2013.
11) Welford RW, Garzotti M, Lourenco CM, Mengel E, Marquardt T, et al: Plasma lysosphingomyelin demonstrates great potential as a diagnostic biomarker for Niemann−Pick disease type C in a retrospective study. *PLoS One* 9: e114669, 2014.
12) Maekawa M, Jinnoh I, Matsumoto Y, Narita A, Mashima R, et al: Structural determination of lysosphingomyelin-509 and discovery of novel class lipids from patients with Niemann−Pick disease type C. *Int J Mol Sci* 20: 2019, 5018.
13) Sidhu R, Mondjinou Y, Qian M, Song H, Kumar AB, et al: *N*-acyl-*O*-phosphocholineserines: Structures of a novel class of lipids that are biomarkers for Niemann−Pick C1 disease. *J Lipid Res* 60: 1410−1424, 2019.
14) Wilcken B, Wiley V, Hammond J, Carpenter K: Screening newborns for inborn errors of metabolism by tandem mass spectrometry. *New Engl J Med* 348: 2304−2312, 2003.
15) Mashima R, Maekawa M: Lipid biomarkers for the peroxisomal and lysosomal disorders: Their formation, metabolism and measurement. *Biomarkers Med* 12: 83−95, 2018.
16) Carstea ED, Morris JA, Coleman KG, Loftus SK, Zhang D, et al: Niemann-Pick C1 disease gene: Homology to mediators of cholesterol homeostasis. *Science* 277: 227−231, 1997.
17) Naureckiene S, Sleat DE, Lackland H, Fensom A, Vanier MT, et al: Identification of HE1 as the second gene of Niemann−Pick C disease. *Science* 290: 2298−2301, 2000.
18) Kwon HJ, Abi-Mosleh L, Wang ML, Deisenhofer J, Goldstein JL, et al: Structure of N-terminal domain of NPC1 reveals distinct subdomains for binding and transfer of cholesterol. *Cell* 137: 1213−1223, 2009.
19) Reddy JV, Ganley IG, Pfeffer SR: Clues to neuro-degeneration in Niemann−Pick Type C disease from global gene expression profiling. *PLoS One* 1: e19, 2006.
20) Mazzacuva F, Mills P, Mills K, Camuzeaux S, Gissen P, et al: Identification of novel bile acids as biomarkers for the early diagnosis of Niemann−Pick C disease. *FEBS Lett* 590: 1651−1662, 2016.
21) Slotte JP: Biological functions of sphingomyelins. *Prog Lipid Res* 52: 424−437, 2013.
22) Saigusa D, Okamura Y, Motoike I, Katoh Y, Kurosawa Y, et el: Establishment of protocols for global metabolomics by LC-MS for biomarker discovery. *PLoS One* 11: e0160555, 2016.
23) Sato T, Kawasaki Y, Maekawa M, Takasaki S, Saigusa D, et al: Value of global metabolomics in association with diagnosis and clinicopathological factors of renal cell carcinoma. *Int J Cancer* 145: 484−493, 2019.
24) Kikuchi K, Saigusa D, Kanemitsu Y, Matsumoto Y, Thanai P, et al: Gut microbiome-derived phenyl sulfate contributes. *Nat Commun* 10: 1835, 2019.
25) Wiklund S, Johansson E, Sjölström L, Mellerowicz EJ, Edlund U, et al: Visualization of GC/TOF-MS-based metabolomics data for identification of biochemically interesting compounds using OPLS class models. *Anal Chem* 80: 115−122, 2008.
26) Giese AK, Mascher H, Grittner U, Eichler S, Kramp G, et al: A novel, highly sensitive and specific biomarker for Niemann-Pick type C1. *Orphan J Rare Dis* 10: 78, 2015.

27) Guan Z, Li S, Smith DC, Shaw WA, Raetz CRH: Identification of *N*-acylphosphatidylserine molecules in eukaryotic cells. *Biochemistry* 46: 14500−14513, 2007.
28) Wood PL: Accumulation of *N*-acylphosphatidylserines and *N*-acylserines in the frontal cortex in schizophrenia. *Neurotransmitter* 1: e263 (2014).
29) Makinoshima H, Umemura S, Suzuki A, Nakanishi H, Maruyama A, et al: Metabolic determinants of sensitivity to phosphatidylinositol 3-kinase pathway inhibitor. *Cancer Res* 78: 2179−2191, 2018.